Supplemental Information for:

Plasma-treated gold microelectrodes for subsecond detection of Zn(II) with fast-scan cyclic voltammetry

Anntonette N. Perry[1], Romana Jarosova[1], Colby E. Witt[1], Moriah E. Weese-Myers[1], Vivek Subedi[1], Ashley E. Ross[1,2]

[1]University of Cincinnati
Department of Chemistry
312 College Dr.
404 Crosley Tower
Cincinnati, OH 45221-0172

Office# 418A Rieveschl
Email: Ashley.ross@uc.edu
[2]Corresponding Author

Keywords: electrochemistry, gold fibers, metals, metallotransmitters, cyclic voltammetry, gold cleaning

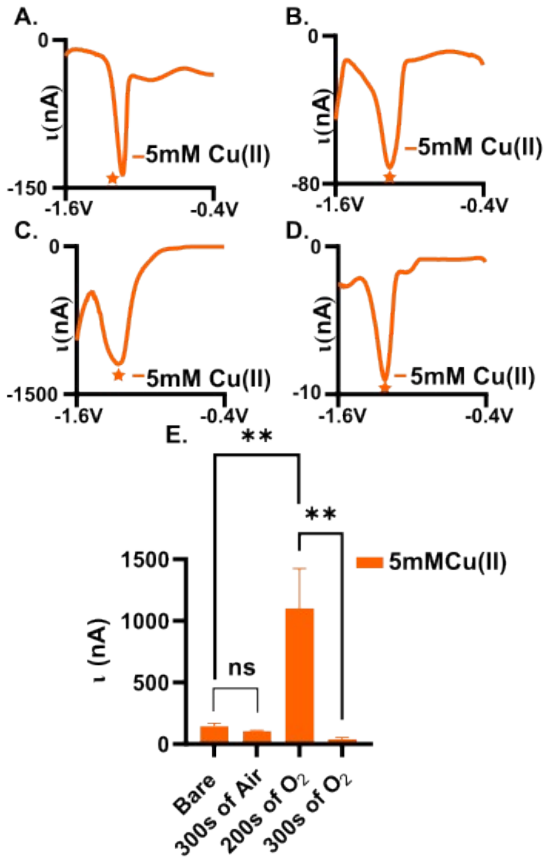

Figure S1: Cu(II) adsorbs to the surface of AuME regardless of treatment. Measurements were made using 5 mM Cu(II) in 1M KCl. (A) On untreated fibers and (B) air plasma treated fibers, Cu(II) shows a reduction peak of -1.3 V, similar to Zn(II). (C) Oxygen plasma treated gold fibers (treatment was for 200 s). The reduction peak is observed at -1.4 V: a slight shift from the air plasma and untreated electrodes. (D) Longer treatments times with oxygen plasma (300 s) resulted in less observable current for Cu(II) reduction. (E) Comparison of treatments show high current for the optimized treatment of 200s of oxygen plasma.

A. Bare fiber

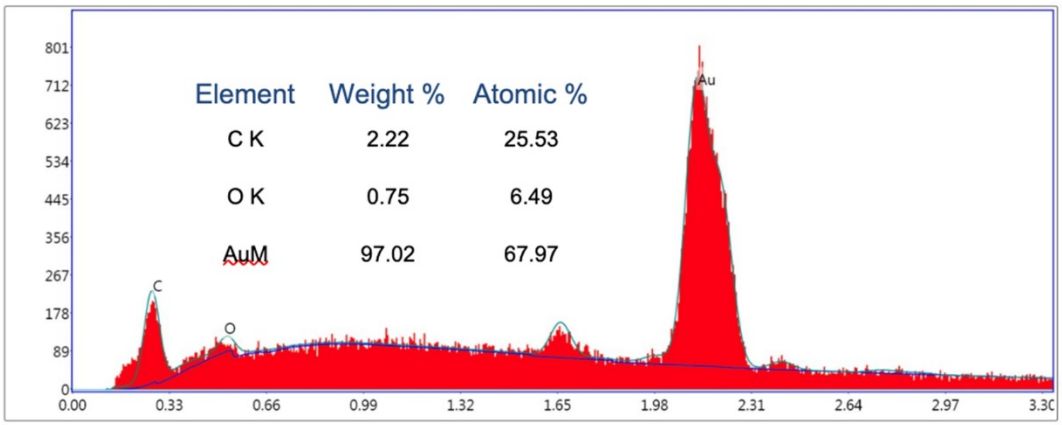

Lsec: 30.0 0 Cnts 0.000 keV Det: Octane Super Det

B. 200s O_2 plasma

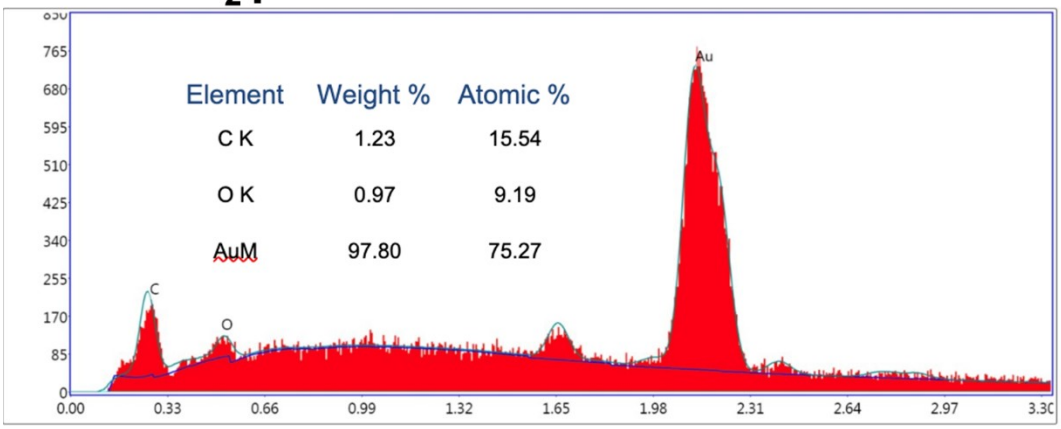

Figure S2: EDAX shows elemental changes to the surface validating impurities and oxygen addition. (A) Bare gold fiber shows peaks inherent to a homogeneous gold fiber. (B) Oxygen plasma decreases the surface carbon and increases surface oxygen (n=3).

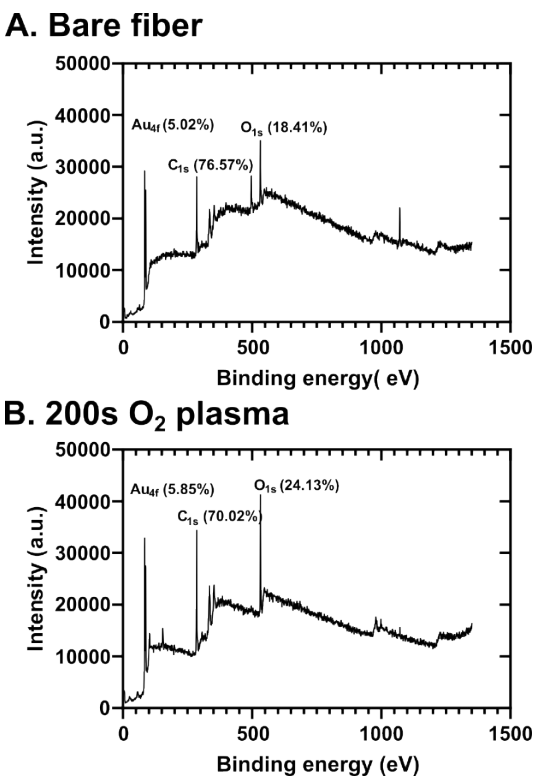

Figure S3: XPS demonstrates changes in carbon and oxygen composition on Au fiber surface. (A) Carbon accounts for 76.5% of surface functionality on untreated fibers, while oxygen accounts for less than 20%. (B) Carbon functionalization decreases and oxygen functionalization increases following treatment with O_2 plasma.

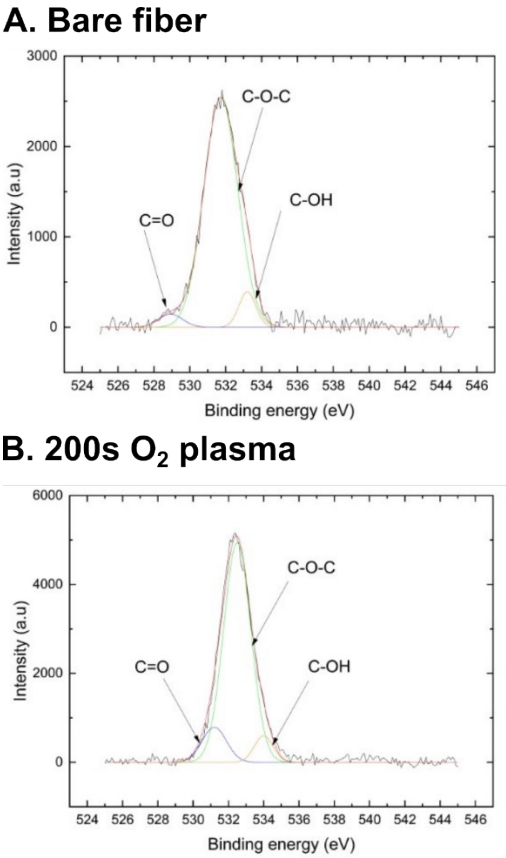

Figure S4: Oxygen surface functionalization changes with O_2 plasma treatment. (A) Bare fibers show minimal C=O functionalization; while (B) plasma treated fibers show substantial increases to C=O content with corresponding decreases to C-OH functional groups.

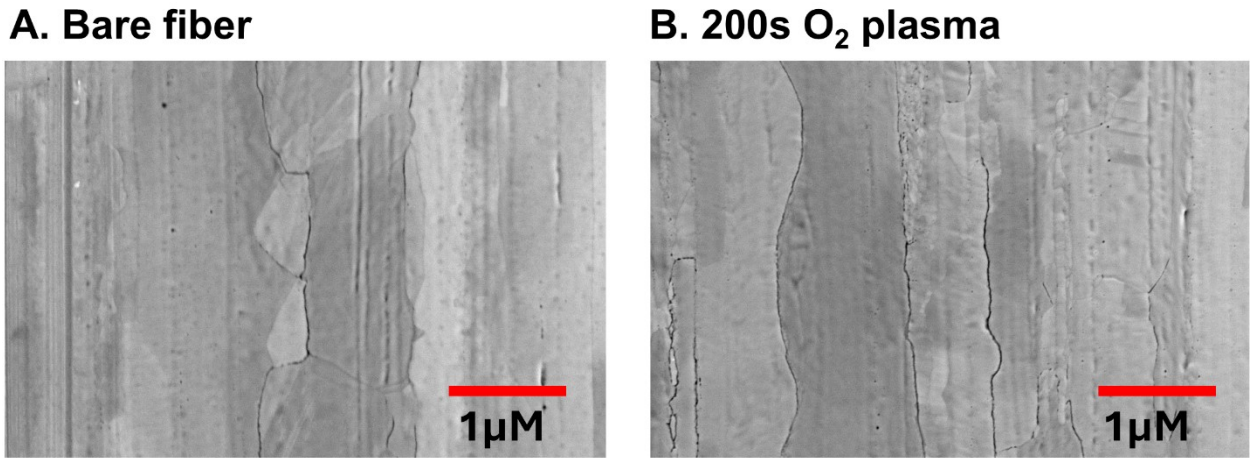

Figure S5: Few morphological changes are evident between bare fibers and optimally O_2- plasma treated fibers. Both bare (A) and treated (B) fibers showed surface defects including pitting and craquelure. These defects were only apparent at high resolutions, whereas extended treatment times showed more visible changes in topology.

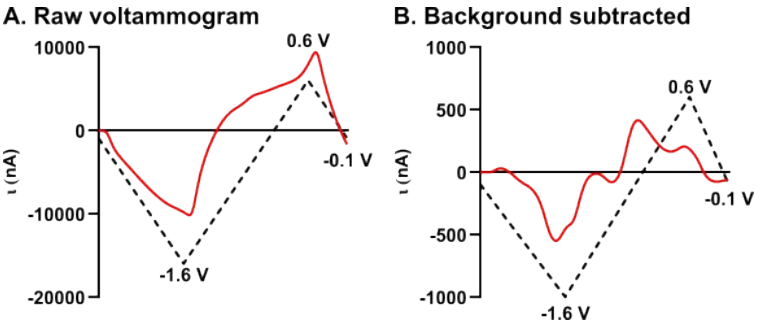

Figure S6: Because of large capacitive currents, micromolar concentrations of Zn(II) are not detectable on a CV pre-background subtraction (A). Background subtraction is performed by averaging 10 scans ~1s pre-injection and setting the average CV obtained equal to zero, eliminating capacitive current and all faradaic current from reactions happening at that time (for example, reduction of oxide functionalities on the electrode surface). After background subtraction, Zn(II) reduction is clearly visible (B).

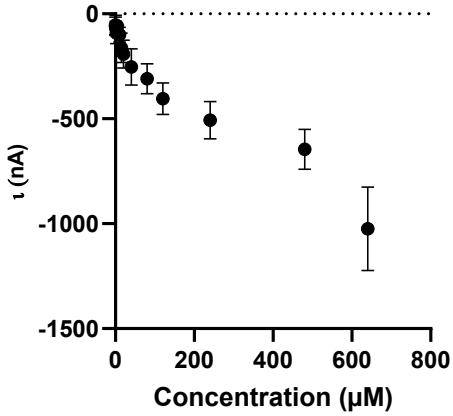

Figure S7: Zn(II) does not reach complete saturation of surface binding sites even at high micromolar concentrations. Concentrations from 100 nM to 640 μM were tested. Current continues to increase at 640 μM and does not flatten indicating that not all surface sites are occupied (n = 4-10).

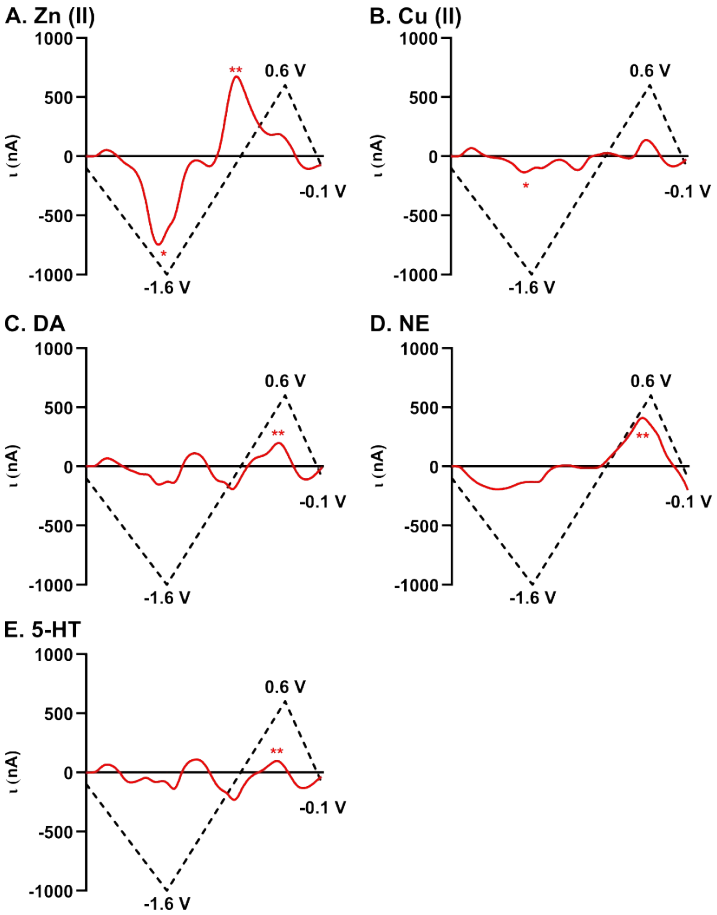

Figure S8: Zn^{2+} does not have any significant biologically relevant interferents at AuFMEs. Clear reduction (*) and oxidation (**) peaks are observable for 20μM Zn (II) at -1.2 V and -0.5 V, respectively. Cu (II) detection was unstable on plasma-treated electrodes; minimal reduction was observed at -1.2 V (B). Dopamine (DA), norepinephrine (NE), and serotonin (5-HT) showed no interference with Zn(II) reduction; NE oxidized at 0.55 V, while minimal interaction was observed for DA and 5-HT (C,D,E). (n = 3)